Short communication

Electrode engineering of nanoparticles for lithium-ion batteries—Role of dispersion technique

T.J. Patey, A. Hintennach, F. La Mantia, P. Novák*

Electrochemistry Laboratory, Paul Scherrer Institut, CH-5232 Villigen PSI, Switzerland

ABSTRACT

The influence of suspension dispersion technique on electrochemical performance of electrodes for lithium-ion batteries is investigated. Anatase TiO$_2$ with particle diameters of 20 nm is used as a model material and is dispersed with carbon black aggregates within an organic solution. Electrode structure is analyzed by scanning electron microscopy (SEM) and the electrochemical performance investigated by electrochemical impedance spectroscopy (EIS) and rate capability experiments. SEM investigations indicate that a conventional mixing technique with a turbo-stirrer disperses the TiO$_2$ and carbon black agglomerates of nanoparticles within an order of 1 μm and not within the primary particle size order lower than 100 nm. EIS experiments show that dispersing the TiO$_2$/carbon black suspensions with a commercial surfactant prior to electrode formation reduces specific impedance and charge transfer resistance of the electrodes. These electrodes are seen to have higher galvanostatic contributions than for electrodes dispersed without the surfactant. Improved break down of the TiO$_2$ agglomerates occurs with more rigorous dispersion techniques and leads to improved electrochemical performance of the electrodes. Dispersion technique is argued to be a critical process in producing high performance electrodes with nanoparticles as active material.

© 2008 Elsevier B.V. All rights reserved.

1. Introduction

Methods of optimizing electrodes for lithium-ion batteries include processing conditions, composite electrode morphology, and binder selection [1–3]. Pre-dispersion of carbon black prior to slurry preparation has been seen to reduce internal resistance and improve electrochemical performance of cathode materials [4,5]. Furthermore, if the carbon black is agglomerated and not uniformly distributed in an electrode, then a bi-modal distribution of local resistances is obtained [6]. Dry carbon black forms agglomerates of nano-sized particles, so pre-dispersion in a liquid slurry prior to electrode formation improves the interparticle contact between active materials. Ensuring interparticle contact has been identified as one of the challenges for use of nanoparticles as active material in lithium-ion batteries [7]. Nanoparticles are often mixed into a slurry from a dry powder state. Van der Waals forces draw individual nanoparticles together to form clumped aggregates and are a challenge to break down so that the nanoparticles can be intermixed with carbon. To overcome this disadvantage, electrical contact between particle/particle and particle/current collector should be ensured by establishing an electrically conductive network of carbon. This would promote full functionalization of nanoparticles for lithium-ion batteries.

TiO$_2$ has shown promise as a negative material in lithium-ion batteries [7–12]. It is safe and well suited for rapid charging and discharging. One drawback to the energy density is that lithium-ion insertion and extraction into and out of the material occur around 1.6 and 2.1 V vs. Li/Li$^+$, respectively, which is relatively high for a negative material. While this is a drawback for commercial use in high energy devices, it is an advantage for use of TiO$_2$ as a model material to investigate electrode engineering as no significant side reactions are expected with the electrolyte within this voltage range.

The structure of anatase TiO$_2$ during lithium-ion insertion is characterized by a phase transition from a tetragonal to an orthorhombic structure [13]. Bulk anatase TiO$_2$ has a theoretical specific charge of 168 Ah kg^{-1}, for lithium-ion insertion into the material, this corresponds to $x = 0.5$ for the reaction:

$$TiO_2 + x(Li^+ + e^-) \rightarrow Li_xTiO_2$$
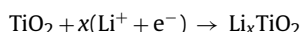
In this work, TiO$_2$ nanoparticles are dispersed in suspensions with carbon black by different mechanisms. These suspensions are mixed into a slurry and prepared into composite electrodes. The electrochemical impedance spectroscopy and rate capability of these electrodes are measured and compared to develop

* Corresponding author. Tel.: +41 56 310 2457; fax: +41 56 310 4415.
E-mail address: petr.novak@psi.ch (P. Novák).

insight on the role of dispersion technique on electrochemical performance.

2. Experimental

Dry powder of anatase TiO_2 (Tronox A-K-1, Kerr-McGee Pigments) with diameters of about 20 nm (SEM) and a specific surface area (SSA) of 90 $m^2 g^{-1}$ is used as the active material (AM). Carbon black (CB, Super P, TIMCAL SA) with an SSA of 62 $m^2 g^{-1}$ was used as an electrically conductive additive and 10 wt.% polyvinylidene fluoride binder (PVDF SOLEF 1015, Solvay) dissolved in N-methylpyrrolidinone (NMP, Fluka).

Analysis by scanning electron microscopy (SEM) was performed with a Zeiss Gemini 1530 (Fig. 1) and also with a Supra Zeiss VP55 (Fig. 2) both operated at 1 kV.

A CB-based model electrode composing of an AM:CB:PVDF mass ratio of 1:8:1 is prepared solely to see if the TiO_2 agglomerates are broken down following the conventional mixing method (Fig. 1).

In this work, agglomerates refer to particles held together by weak, physical van der Waals forces, while aggregates refer to particles held together by stronger chemical or sintering bonds. In literature these are sometimes referred to as soft and hard agglomerates [14], respectively. The CB is seen in Fig. 2 to be composed of aggregates of primary particles physically connected to one another by sintered necks and these aggregates are clumped together into agglomerates. The TiO_2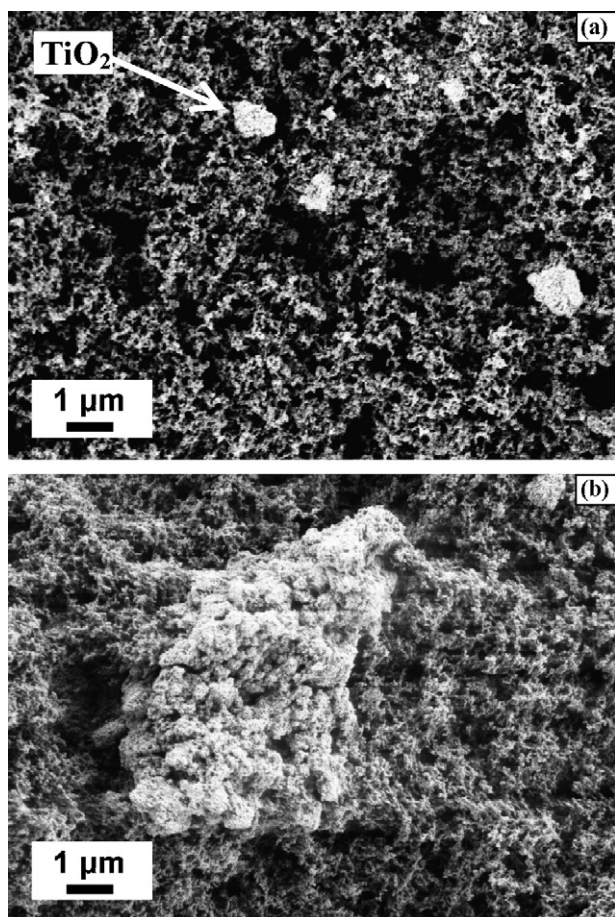 nanoparticles appear to be non-aggregated primary particles held together by van der Waals forces to form agglomerates, as seen in Fig. 1b. In general, the forces holding agglomerates together can be readily broken down by high energy agitation when they are incorporated into a liquid. In contrast, aggregates are held together by more stable bonds and cannot be fragmented appreciably with intense agitation [15].

For electrochemical impedance spectroscopy (EIS) and rate capability experiments, the electrodes contained a AM:CB:PVDF mass ratio of 8:1:1. To demonstrate the importance of homogeneity, three different slurries were prepared differently for three different electrodes. The first slurry was stirred by hand for 2 min. The other two slurries were well mixed by a turbo-stirrer (PT2100, Kinematica) for 5 min at full power. One of these two slurries contained a commercial surfactant, Triton X-100 (Sigma–Aldrich), and it accounted for 0.7 wt.% of the electrode mass. The slurry is spread by doctor-blade at a thickness of 250 μm onto an aluminum foil and dried under vacuum at 110 °C overnight in order to remove the solvent and form a composite electrode.

Electrodes with a diameter of 13 mm were punched out and dried in a vacuum chamber at 120 °C overnight. They were then assembled in test cells similar to coin cells [16] where they function as working electrodes. Lithium metal (Aldrich, 99.9%) was used as both counter and reference electrode. It was separated from the working electrode by a 1 mm thick fiberglass separator soaked in 500 μL of electrolyte (1 M $LiPF_6$ in ethylene carbonate (EC)/dimethyl carbonate (DMC) (1:1 by mass, Ferro GmbH). Cells were assembled in an argon-filled glove box with less than 1 ppm of oxygen, nitrogen, and water contents.

EIS experiments were conducted with an electrochemical workstation (IM6ex, Zahner-Elektrik GmbH). The cells for the EIS experiments contained two uncycled electrodes in a symmetrical arrangement with both TiO_2-based electrodes coming from the same electrode batch. The electrochemical impedance was measured at an affixed DC potential of 0 V with an alternating current in the frequency range of 100 kHz to 10 mHz with a signal amplitude of 10 mV.

Both cyclic voltammetry (CV) and galvanostatic measurements were performed by a computer-controlled cell capture (CCCC) system (Astrol Electronics AG, Oberrohrdorf, Switzerland) in a potential window of 1–3 V vs. Li/Li$^+$. The CV measurements were done at a potential scan rate of 0.1 mV s^{-1}. For the rate capability experiments, the electrodes were cycled galvanostatically in the range of 1–3 V vs. Li/Li$^+$ for varying specific currents proportional to the mass of TiO_2. In order to promote complete discharge/charge at the respective potential limits, a potentiostatic step was included until the specific current was 34 mA g^{-1}.
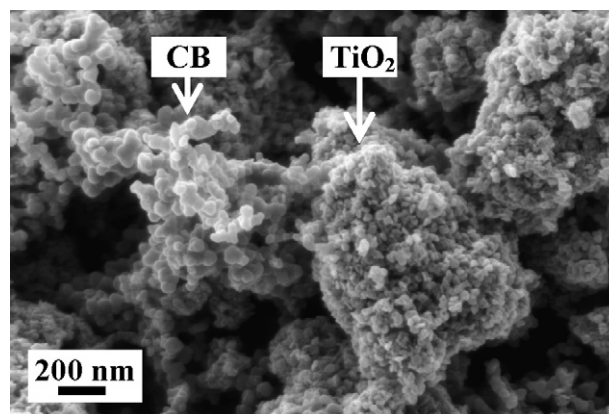

Fig. 1. SEM of a carbon black-based (80 wt.%) model electrode with TiO_2 (10 wt.%) and PVDF (10 wt.%). This is an example of an electrode made from a poorly mixed slurry stirred by a convention dispersion technique. Carbon black particles are the darker-shaded branched aggregates and TiO_2 are the lighter-shaded clumped agglomerates. (a) Prevailing areas of the electrode; (b) a large agglomerate of TiO_2.

Fig. 2. SEM of a TiO_2-based (80 wt.%) model electrode with carbon black (CB, 10 wt.%) and PVDF (10 wt.%). This is an example of an electrode made from a poorly mixed slurry stirred by a convention dispersion technique.

3. Results and discussion

TiO$_2$ is a known semi-conductor [17] and the anatase TiO$_2$ powder used in this work is measured to have an electrical resistivity of about 250 kΩ m under a 5 kg weight in a disc-shaped, plastic mold 10 mm in diameter. This value indicates that electrical conductivity is likely a limiting step for the electrochemical performance, which qualifies TiO$_2$ as a suitable model material for investigating the importance of dispersion technique on electrochemical performance.

To develop a qualitative overview of the ability of the conventional stirring method in breaking down TiO$_2$ agglomerates, SEM images were taken of the carbon-based electrode with 10 wt.% TiO$_2$ (Fig. 1). In the image of Fig. 1a, lighter-shaded agglomerates of TiO$_2$ nanoparticles are seen intermixed within a matrix of darker-shaded carbon black aggregates. The TiO$_2$ agglomerate sizes are in the order of 1 μm. This indicates that the conventional stirring technique is insufficient to overcome the surface forces drawing the TiO$_2$ nanoparticles of 20 nm diameters together. Furthermore, a couple of TiO$_2$ agglomerates with sizes much greater than 1 μm were noticed, with an example seen in Fig. 1b.

Fig. 2 shows an SEM image of a standard TiO$_2$-based (80 wt.%) model electrode. Here, the TiO$_2$ agglomerate size is harder to estimate than in Fig. 1, but the quality of the mixing of carbon black and TiO$_2$ is still possible to evaluate. In Fig. 2, agglomerates of TiO$_2$ nanoparticles are mixed with agglomerates of carbon black aggregates. Each material is agglomerated with itself, and mixing of individual primary particles with the other material is not seen. The observations of SEM images in Figs. 1 and 2 can be summarized as follows: mixing of TiO$_2$ and carbon black occurs, but it appears to occur at a scale in the order of 1 μm and not in the scale of the primary particle sizes of both materials (less than 100 nm). This is a strong indication that the conventional mixing process can be improved and a motivation for development and analysis of dispersion techniques.

To improve upon the conventional mixing technique, a commercial surfactant (Triton X-100) was used to improve dispersion of the suspensions of TiO$_2$ and carbon black. This has been seen to disperse agglomerates of TiO$_2$ nanoparticles with particle diameters of 0.23 μm in aqueous solutions to improve colloidal stability and decrease agglomerate size [18]. Three model electrodes were made for electrochemical evaluation, each from slurries dispersed with different techniques. One slurry was hand-stirred, one turbo-stirred, and another turbo-stirred with a pre-dispersion of the TiO$_2$/carbon black suspension with Triton X-100. These are the three candidate electrodes used in this work to investigate the role of the dispersion technique. Although many other techniques exist, these three were selected as it was suspected that their influence on the electrochemical performance would be significant.

Fig. 3 displays the Nyquist plots for the EIS experiments on the TiO$_2$-based electrodes. The semicircles in the medium to high frequency range are seen in the inset of Fig. 3. The high frequency ends of the curves confirm no significant difference in the ohmic cell-electrolyte resistance, as expected. However, the electrode prepared with the surfactant has a lower mass specific impedance in the low frequency region, and therefore likely a higher surface area in contact with the electrolyte as seen in the inset of Fig. 3. The improved dispersion of TiO$_2$ nanoparticles with the carbon black led to a decrease in the overall charge transfer resistance and a less distorted semicircle in the high frequency region, thus indicating the better contact between particles (lower electronic resistance of the electrode) and also higher surface area in contact with the electrolyte. The TiO$_2$-based electrode made from the hand-stirred slurry had the highest overall resistance to charge transfer and also the strongest distortion in the high frequency semicircle, indi-
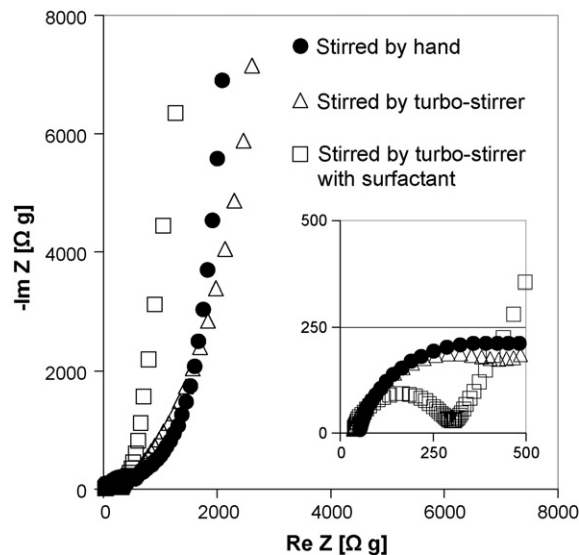

Fig. 3. Nyquist plot of three electrodes. Mass is calculated for TiO$_2$ present in the electrodes.

cating that the electronic resistance of the electrode is relatively high and that there is lower surface area in contact with the electrolyte. These effects are attributed to the poor dispersion of the TiO$_2$ nanoparticles and carbon black. The turbo-stirred electrode without surfactant has the same surface area in contact with the electrolyte as the hand-stirred electrode, but the lower distortion of the high frequency semicircle suggests better electronic contact between the particles. EIS data suggest that a significant improvement of the electrochemical performances should be observed when a surfactant is appropriately used. Some improvement of the electrochemical performances should be observed also by turbo-stirring the slurry.

Cyclovoltammetry (figure not shown) of TiO$_2$ was measured to have oxidative and reductive peaks at about 2.1 and 1.6 V vs. Li/Li$^+$, respectively. Therefore, potential limits of 1 and 3 V vs. Li/Li$^+$ were selected to promote complete charge and discharge of the material in the galvanostatic rate capability experiments.

Fig. 4 illustrates the results of the rate capability experiments of the three TiO$_2$-based electrodes. This highlights the importance of the dispersion technique when the active material is composed of non-aggregated nanoparticles clumped into agglomerates. The sum of galvanostatic and potentiostatic discharge (lithium-ion insertion) capacity is seen to be approximately the same for each electrode in the discharge capacity bar graph in Fig. 4a. Consideration of the galvanostatic contribution illustrates the effect of electrode engineering: the better the dispersion technique, the higher the galvanostatic contribution at C-rates greater than 1. The sum of galvanostatic and potentiostatic contributions, however, remains constant, confirming that the total specific charge which can be stored in each electrode is about the same. The electrode dispersed with the surfactant has noticeably the highest galvanostatic contribution and the most significant improvement in performance is at 5 C-rate, as deduced from the EIS data. The advantage of the turbo-stirred method over the hand-stirred dispersion is also apparent at C-rates greater than 1. Better dispersions lead to better mixing of TiO$_2$ nanoparticles and carbon black aggregates which could be due to break down of the agglomerates of both materials to smaller sizes. Analysis of the charge (lithium-ion extraction) capacity bar graph in Fig. 4b is in agreement with the same observations of Fig. 4a: better dispersions lead to improved electrochemical performance. Of interest is that the galvanostatic
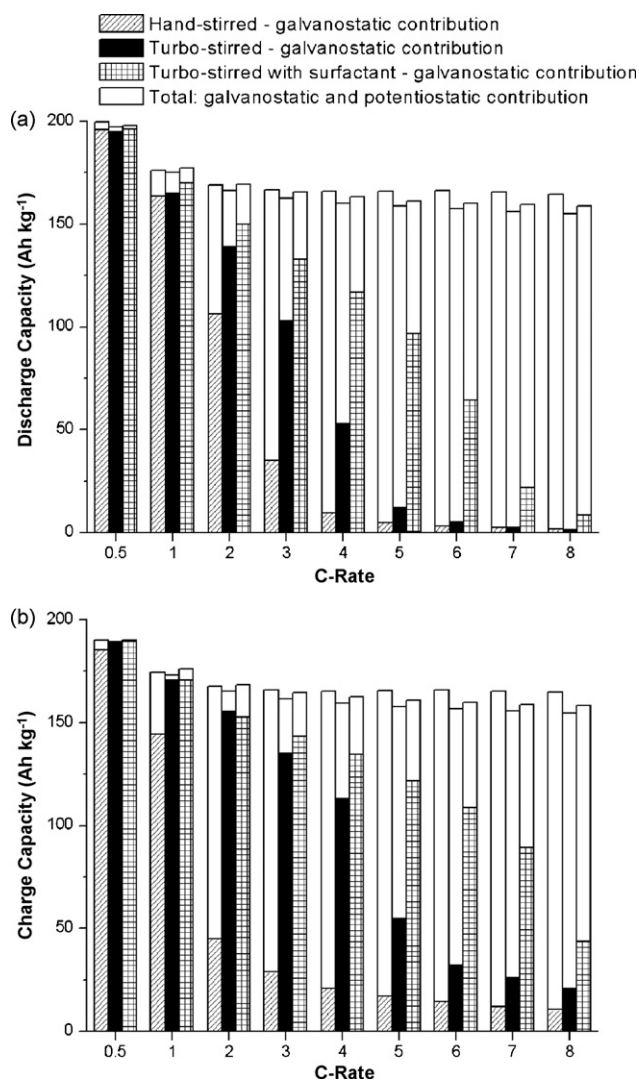
Fig. 4. Discharge [(a), Li-ion insertion] and charge [(b), Li-ion extraction] capacities per unit mass of TiO_2 in composite electrodes. Cycling was performed between 1 and 3 V for various C-rates, where $1C = 168\,mA\,g^{-1}$. Capacity at each C-rate is the average of five cycles.

contribution in the charge capacity bar graph does not decline with the C-rate as much as in the discharge capacity bar graph. These experiments show that the kinetics of lithium-ion extraction is more rapid than lithium-ion insertion into the TiO_2 structure.

It could be argued that the addition of a surface-active agent has a detrimental effect on the interfacial resistance and stability, however, this has not been noticed in this work. This effect is obviously not noticeable because the electrode contained only 0.7 wt.% of Triton X-100, the voltage during cycling did not increase positive to 3 V, and no significant decrease in charge capacity is seen in the rate capability experiments illustrated in Fig. 4. Higher wt.% or higher voltages or both could possibly lead to detrimental Li-Triton X-100 interactions.

The results of the capacity cycling experiments are in agreement with the electrochemical impedance spectroscopy results in Fig. 3 where better dispersions led to lower mass specific impedances. Improved dispersion techniques of TiO_2 nanoparticles 20 nm in diameter and carbon black aggregates lead to a lower overall charge transfer resistance and lower electronic resistance of the electrode, and as a consequence, higher galvanostatic discharge and charge capacities.

4. Conclusions

A need for increasing the electrode's homogeneity by improving the conventional mixing technique was identified by the SEM investigations. These investigations indicate that mixing of agglomerates of both TiO_2 nanoparticles and carbon black aggregates occurs at an order of magnitude of 1 μm, and not below 100 nm. The importance of improved dispersion techniques is illustrated by the electrochemical performances of the TiO_2-based electrodes prepared from TiO_2 and carbon black dispersed by different techniques. The electrode prepared from a suspension with a surfactant was seen to have a lower mass specific impedance and charge transfer resistance and a higher galvanostatic charge/discharge contribution than electrodes from suspensions stirred without the surfactant. The improved dispersion likely led to an electrode with a more homogeneous TiO_2/carbon black distribution, leading to improved electrical contact between smaller TiO_2 agglomerates and the carbon black. These results present an important parameter for the commercialization of nanoparticles for high power lithium-ion batteries. This work does not present an optimized electrode, but demonstrates the importance of homogeneity if nanoparticles are to be used effectively for lithium-ion batteries.

References

[1] B. Lestriez, E. Ligneel, D. Guy, D. Guyomard, in: S.S. Zhang (Ed.), Advanced Materials and Methods for Lithium-Ion Batteries, Transworld Research Network, 2007, pp. 229–256.
[2] R. Dominko, M. Gaberscek, J. Drofenik, M. Bele, S. Pejovnik, J. Jamnik, J. Power Sources 119 (2003) 770–773.
[3] G. Liu, H. Zheng, A.S. Simens, A.M. Minor, X. Song, V.S. Battaglia, J. Electrochem. Soc. 154 (2007) A1129–A1134.
[4] S. Kuroda, N. Tobori, M. Sakuraba, Y. Sato, J. Power Sources 119 (2003) 924–928.
[5] E. Ligneel, B. Lestriez, O. Richard, D. Guyomard, J. Phys. Chem. Solids 67 (2006) 1275–1280.
[6] A.S. Skapin, M. Gaberscek, R. Dominko, M. Bele, J. Drofenik, J. Jamnik, Solid State Ionics 167 (2004) 229–235.
[7] P.G. Bruce, B. Scrosati, J.M. Tarascon, Angew. Chem. Int. Ed. 47 (2008) 2930–2946.
[8] G. Armstrong, A.R. Armstrong, P.G. Bruce, P. Reale, B. Scrosati, Adv. Mater. 18 (2006) 2597–2600.
[9] B. Erjavec, R. Dominko, P. Umek, S. Sturm, S. Pejovnik, M. Gaberscek, J. Jamnik, Electrochem. Commun. 10 (2008) 926–929.
[10] A.R. Armstrong, G. Armstrong, J. Canales, R. Garcia, P.G. Bruce, Adv. Mater. 17 (2005) 862–865.
[11] L. Kavan, M. Kalbac, M. Zukalova, I. Exnar, V. Lorenzen, R. Nesper, M. Graetzel, Chem. Mater. 16 (2004) 477–485.
[12] L. Kavan, M. Gratzel, J. Rathousky, A. Zukal, J. Electrochem. Soc. 143 (1996) 394–400.
[13] L.J. Hardwick, M. Holzapfel, P. Novák, L. Dupont, E. Baudrin, Electrochim. Acta 52 (2007) 5357–5367.
[14] S. Tsantilis, S.E. Pratsinis, Langmuir 20 (2004) 5933–5939.
[15] G.D. Ulrich, Chem. Eng. News 62 (1984) 22–29.
[16] P. Novák, W. Scheifele, F. Joho, O. Haas, J. Electrochem. Soc. 142 (1995) 2544–2550.
[17] M.D. Earle, Phys. Rev. 61 (1942) 56–62.
[18] Z.M. Yaremko, N.H. Tkachenko, C. Bellmann, A. Pich, J. Colloid Interface Sci. 296 (2006) 565–571.